Electronic Supplementary Material (ESI) for Chemical Science.

Electronic Supplementary Information

Unveiling the interplay between homogeneous and heterogeneous catalytic mechanisms in copper-iron nanoparticles working under chemically relevant tumour conditions

Javier Bonet-Aleta[a, b, c, f], Miguel Encinas-Gimenez[a, b, c, f], Esteban Urriolabeitia[d], Pilar Martin-Duque[b, e, f, g, h], Jose L. Hueso*[a, b, c, f], Jesus Santamaria*[a, b, c, f]

This document includes:

Figures ESI-1 to ESI-17
Tables ESI-1 to ESI-7

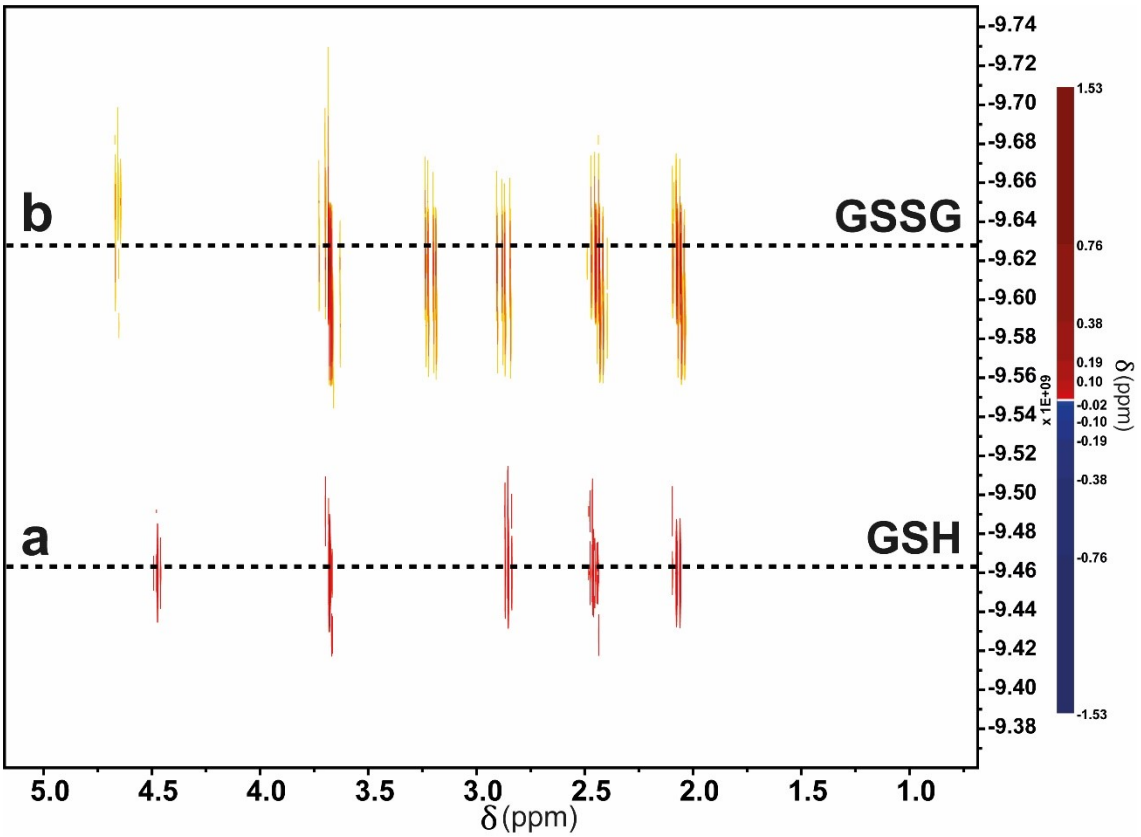

Figure ESI-1. DOSY spectra of (a) GSH and (b) GSSG standards. Molecular size differences between reduced (GSH) and oxidized GSH (GSSG) translate into different diffusion coefficients (D) of the molecule. Following this trend, determined D for GSH is larger in comparison to GSSG.

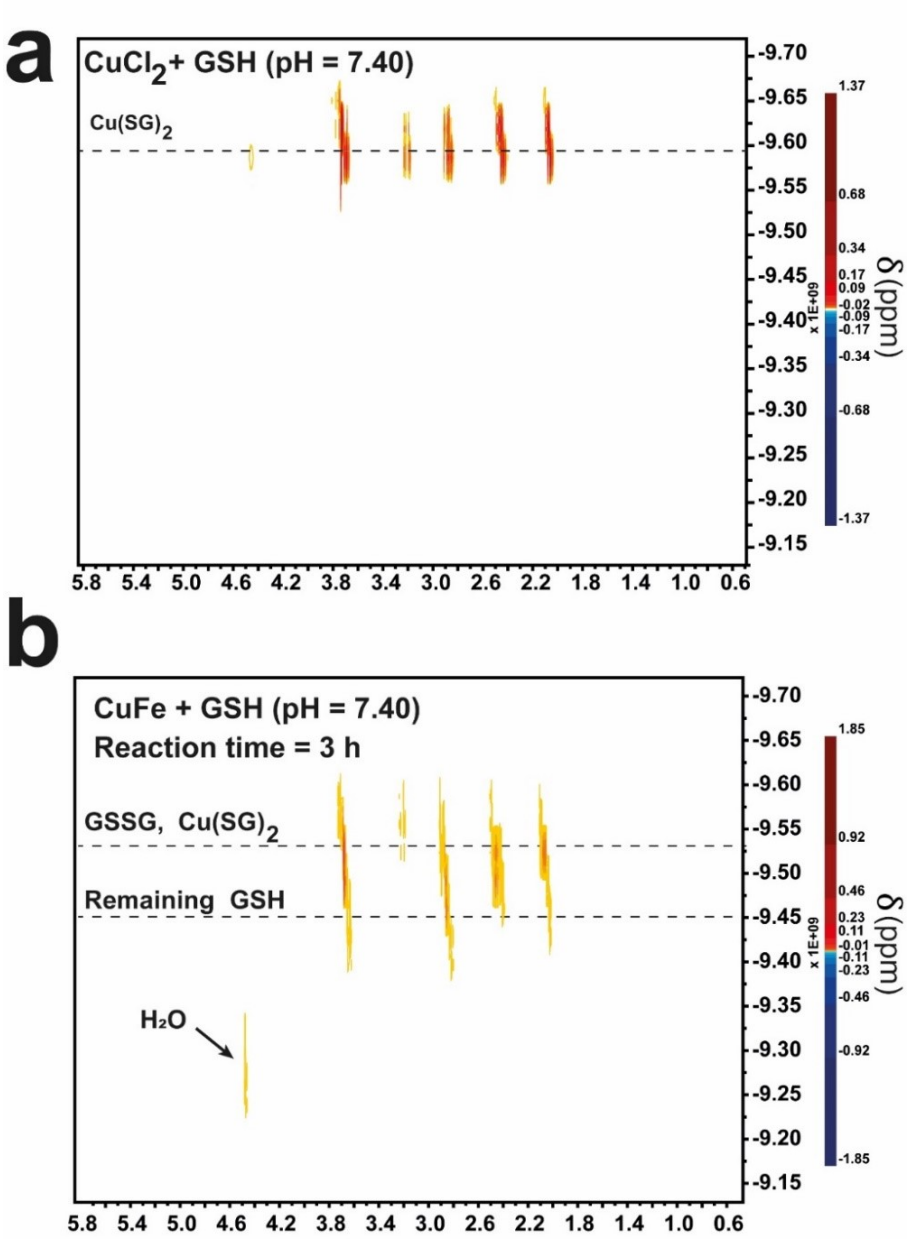

Figure ESI-2. Comparison of diffusion coefficients of (a), $CuCl_2$+GSH (red) and (b) CuFe+GSH (3h) (purple). Reaction conditions [GSH] = 20 mM, pH = 7.0 (HPO_4^{2-}/H_2PO_4), T = 25 ºC, reaction time = 3h. (a) DOSY spectra corresponding to the mixture $CuCl_2$ + GSH indicate the generation of $Cu(SG)_2$ complex and GSSG, which possess a similar molecular size and therefore a similar D is obtained. (b) DOSY spectra of CuFe+GSH reaction at pH = 7.40 at 3h. As reaction is not over at this time, some remaining GSH appears at low D values (highlighted in dashed line). Moreover, as GSH and GSSG/$Cu(SG)_2$ possess same signals for some H (δ=3.70 ppm, δ= 2.85 ppm, δ=2.45 ppm and δ=2.05 ppm), DOSY signals appear wider. A similar signal with a calculated D of $4.00 \cdot 10^{-10}$ $m^2 \cdot s^{-1}$ in comparison with $CuCl_2$+GSH mixture is obtained under conditions that favour leaching of Cu, suggesting the formation of $Cu(SG)_2$ complex in situ using the Cu released from the nanoparticle.

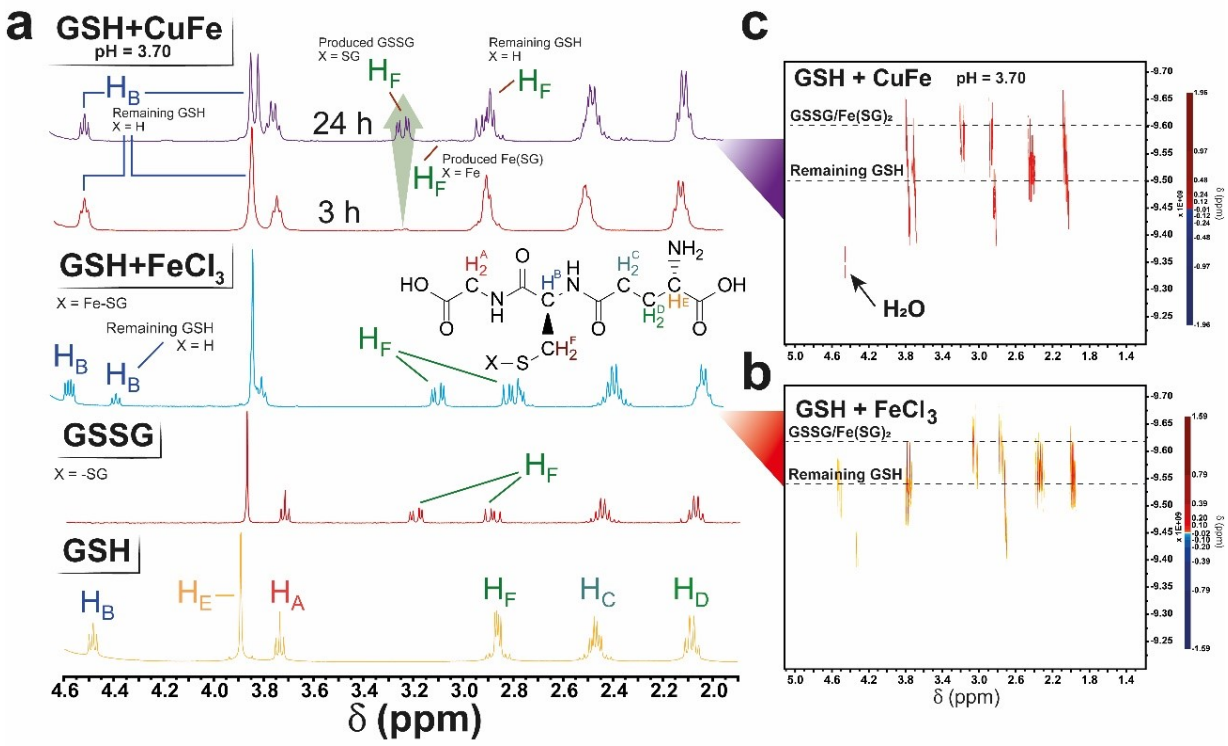

Figure ESI-3. (a) ^{1}H-NMR analysis from $FeCl_3$+GSH experiments. Generation of Fe-SG complex entails the splitting of HF signals at 3.04 and 2.76 ppm. Analysis of reaction supernatant at 3 h reveals a small amount of GSSG produced in comparison with CuFe+GSH at pH = 7.40 consequence of slower reaction kinetics of Fe-homogeneous catalysis of GSH oxidation. However, after 24 h of reaction, a larger amount of Cu has been released and the reaction rate increases. (b) DOSY analysis of GSH+$FeCl_3$ mixture reveals the formation of a product with a D close to GSSG, while an important amount of GSH is still present in the solution (confirmed by ^{1}H-NMR in Fig. S3a). (c) DOSY spectra of CuFe+GSH at pH = 3.70.

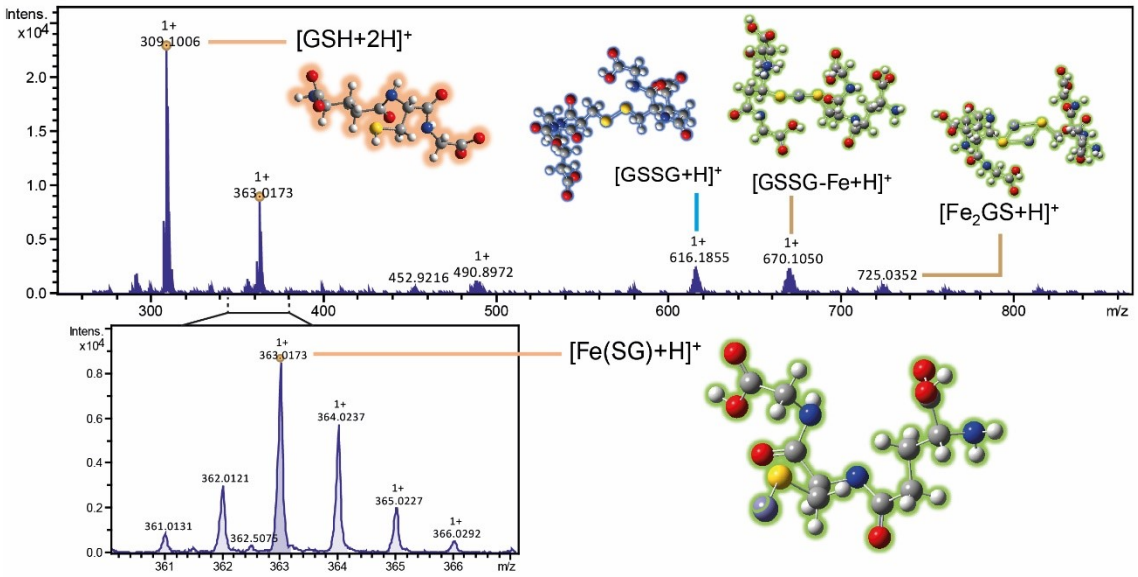

Figure ESI-4. HRMS-ESI analysis of different species found in $FeCl_3$+GSH mixture (pH = 3.60). Remaining GSH is found at m/z = 309.1006 ($[GSH+H]^+$), which is consistent with an important fraction of GSH still present in the solution detected by ^{1}H-NMR (Fig. S3). $[Fe(SG)_x]$ complexes are detected at m/z = 363.0173 ($[Fe(SG)+H]^+$) and m/z=670.1050 ($[Fe(GSSG)+H]^+$ Polynuclear species are also detected at 725.0352 ($[(Fe(SG))_2+H]^+$.

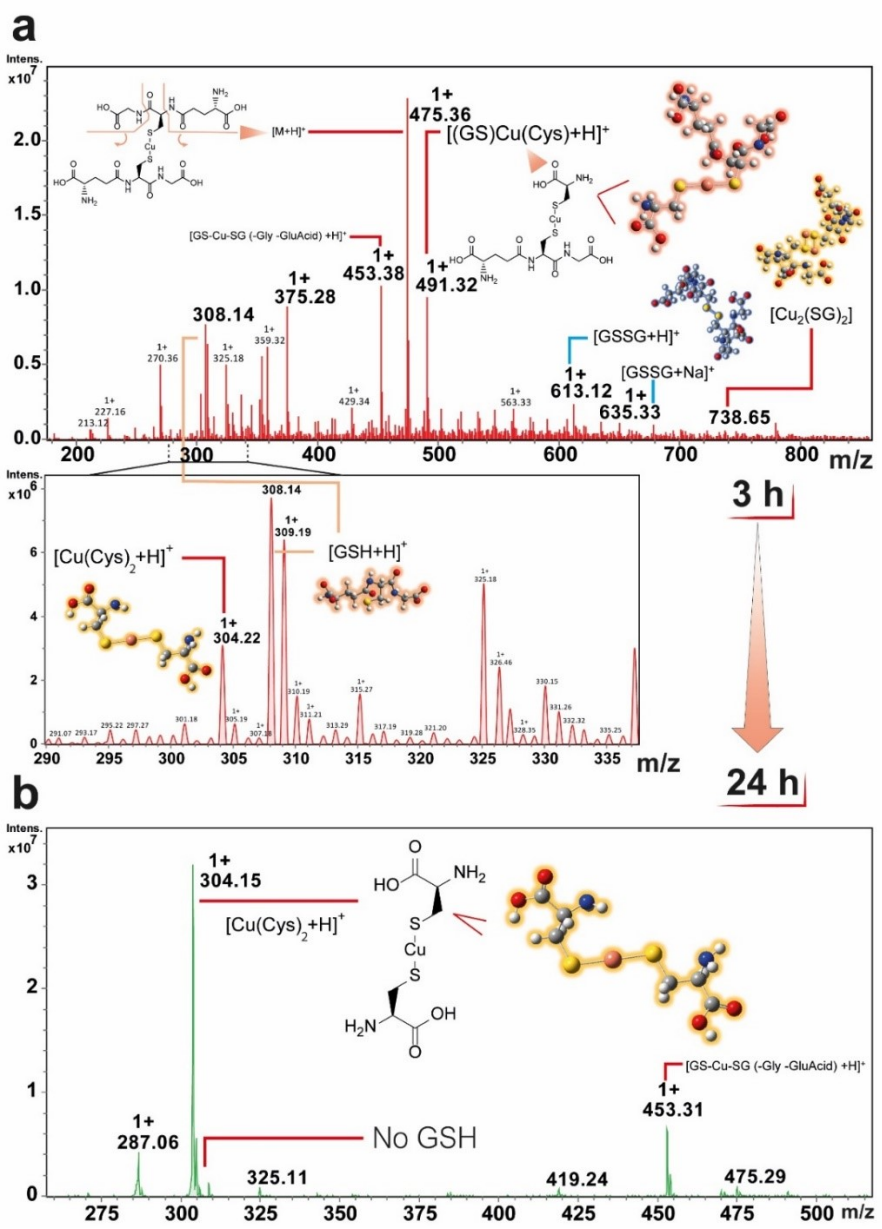

Figure ESI-5. MS-ESI analysis of CuFe+GSH (pH = 7.40) at different reaction times: (a) 3h and (b) 24h. After 3 hours of reaction unreacted GSH and reaction product, GSSG signals at m/z = 308 and m/z = 613 are present in the spectra, in agreement with ^{1}H-NMR results. Different fragments from the $[Cu(SG)_2]+$ complex were found at m/z = 491.32 ($[Cu(SG)(Cys)]^+$), 453.38 ($[Cu(SG)(SG)$-Glutamic Acid-Glycine$]^+$) and 304.27 $[Cu(Cys)_2]^+$, with the Cu-S bond always present. Analysis of the reaction supernatant at reaction time 24 h revealed the total consumption of GSH, according to ^{1}H-NMR analysis and the prominence of the $[Cu(Cys)_2]^+$ fragment. We assume that the nanoparticle affects to the MS fragmentation pattern, as we were not able to detect those fragments by ^{1}H-NMR.

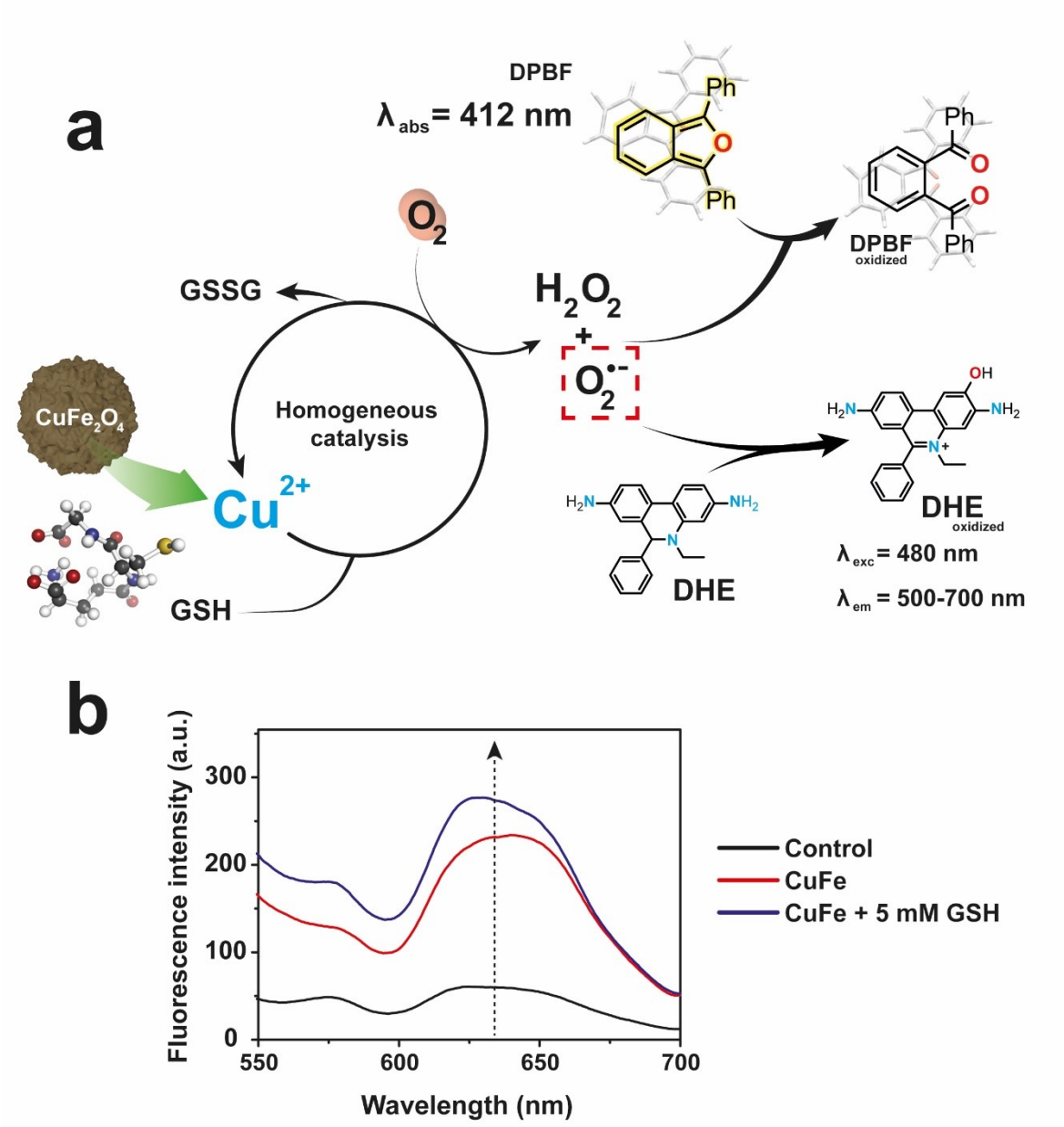

Figure ESI-6. (a) Scheme of the reaction mechanisms to detect ROS species formed when Cu2+ ions are released from the CuFe NPs upon interaction with GSH molecules: DPBF probe detects several ROS species (i.e. H_2O_2 and $\bullet O_2^-$) while Dihydroethidine (DHE) selectively reacts with $\bullet O_2^-$ species to yield a fluorescent adduct (2-hydroxyethidium cation) in the range λ_{exc} = 480 nm/ λ_{em} = 500-700 nm; DPBF absorbs at 412 nm, is oxidized to 1,2-dibenzoylbenzene, a colorless molecule; (b) Fluorescence spectra after 30 minutes of reaction which shows a 20% larger fluorescence signal of DHE oxidized in the presence of 5 mM of GSH due to the generation of $\bullet O_2^-$. Reaction conditions: T = 25°C, pH = 7.4 (adjusted with Na_2HPO_4/KH_2PO_4 buffer), $[DHE]_0$ = 100 µM, [CuFe] = 0.1 mg·mL^{-1}, $[GSH]_0$=5 mM.

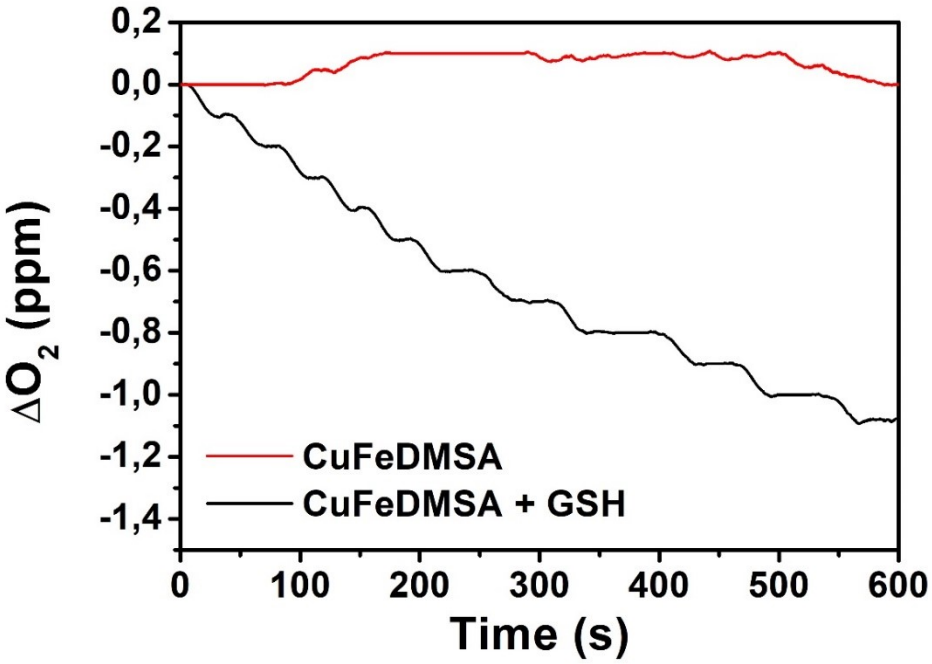

Figure ESI-7. O_2 consumption in the presence of CuFe with or without the addition of 5 mM GSH. [CuFe] = 0.1 mg·mL^{-1}, pH = 7.40 (adjusted with $HPO_4^{2-}/H_2PO_4^-$). The decrease of O_2 levels in solution once CuFe and GSH are mixed corresponds to its role as electron acceptor in the homogeneous GSH oxidation.

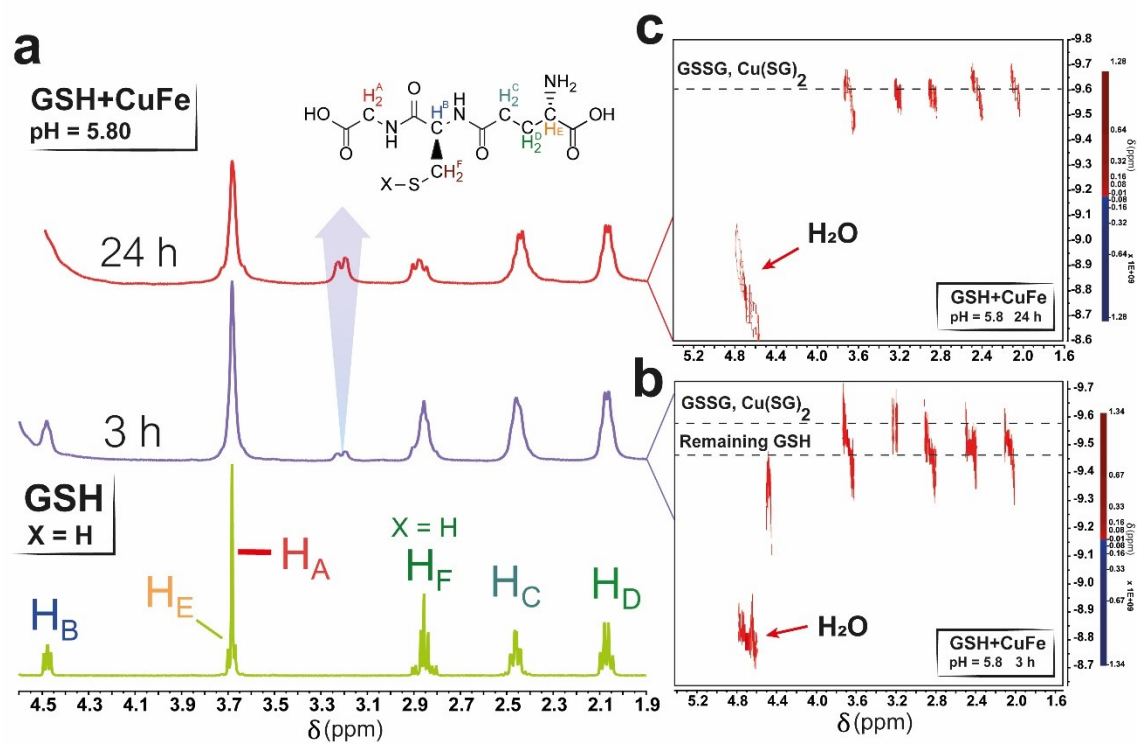

Figure ESI-8. (a) ^{1}H-NMR analysis from CuFe+GSH experiments at pH = 5.80. A similar behavior in comparison with CuFe+GSH at pH = 7.40 is found at tumor-characteristic pH. After 3h of reaction, a characteristic signal of GSSG/Cu(SG)$_2$ at 3.22 ppm appears as consequence of modification of -CH_2- close to -SH group. The reaction is complete after 24 h, as no signal of GSH is present at 4.5 ppm; (b) DOSY spectra of GSH+CuFe mixture at pH = 5.80 (HPO_4^{2-}/$H_2PO_4^-$), presenting both signals from GSH and GSSG/Cu(SG)$_2$; (c) DOSY spectra of GSH+CuFe (pH = 5.8) after 24 h of reaction, with the signal of GSH disappeared. Molecular species with a D similar to GSSG/Cu(SG)$_2$ are detected after 24 hours of reaction.

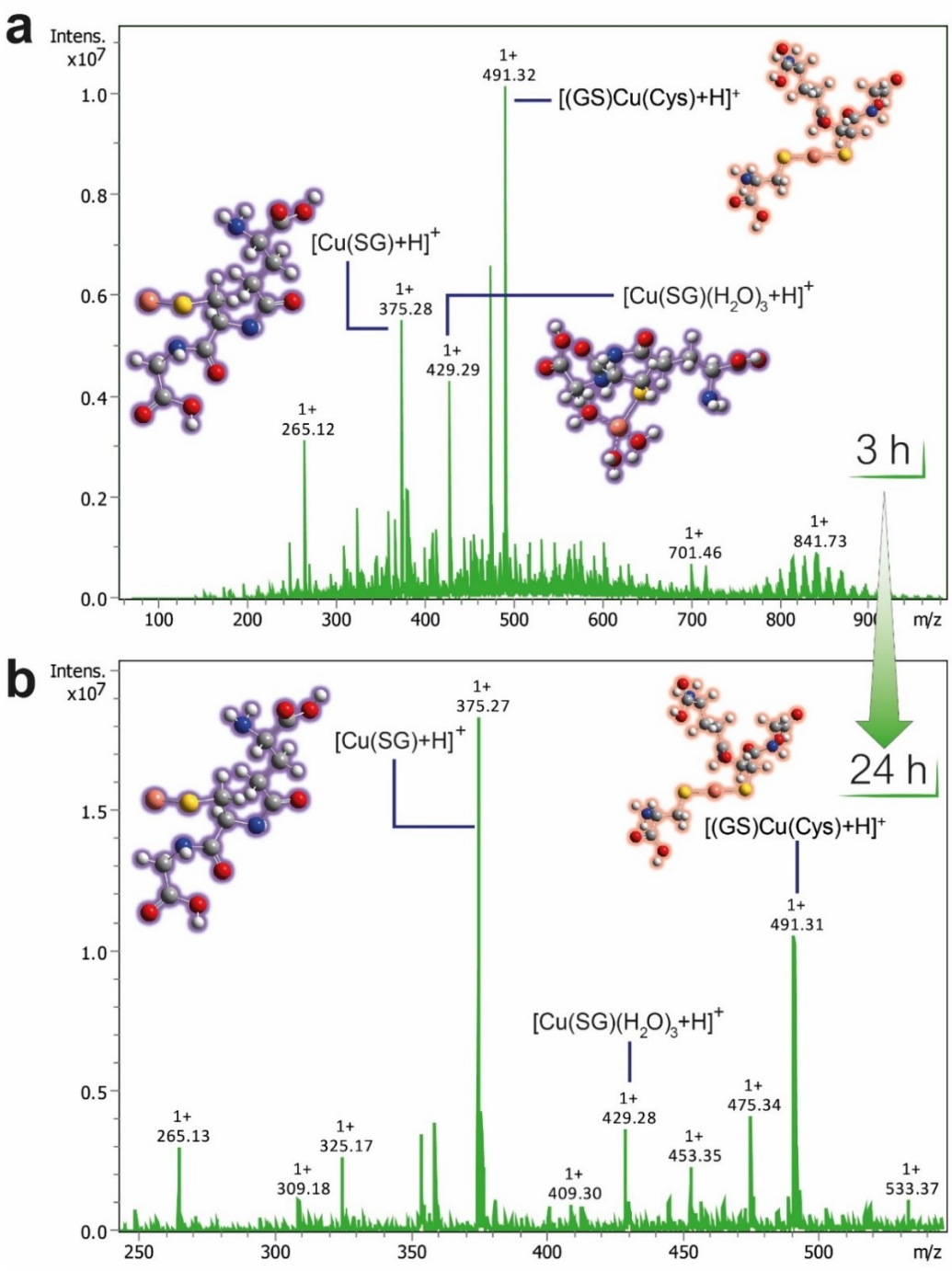

Figure ESI-9. MS-ESI analysis of CuFe+GSH (pH = 5.80) at reaction time (a) 3h and (b) 24h. $[Cu(SG)_2]^+$-derived fragments are present at m/z = 375.28 ($[Cu(SG)+H]^+$), 429.29 ($[Cu(SG)(H_2O)_3+H]^+$) and 491 ($[Cu(SG)(Cys)+H]^+$. Analysis of the reaction supernatant at reaction time 24 h revealed the total consumption of GSH, according to ^{1}H-NMR analysis and the prominence of a [Cu(SG)] fragment.

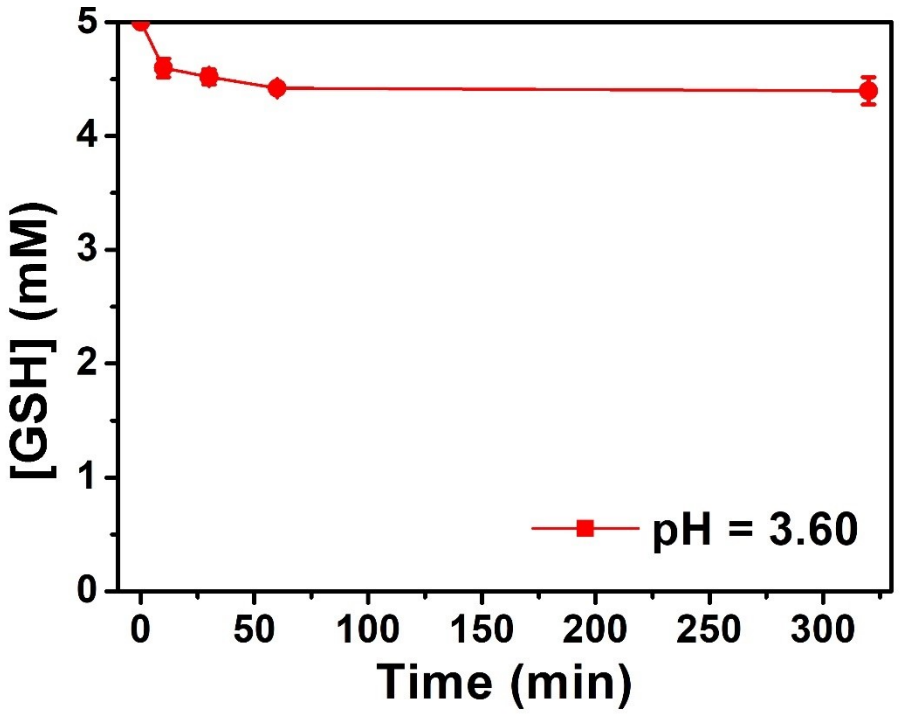

Figure ESI-10. Monitoring of GSH levels at pH = 3.60 in the presence of CuFe catalyst, showing a slight decrease in GSH concentration (in comparison with reaction at pH = 5.80 or 7.40) at early reaction time (320 minutes). Results are in agreement with ^{1}H-NMR/DOSY experiments (Figures ESI-3a-c) indicating that GSH was present in the reaction after 3 h of reaction.

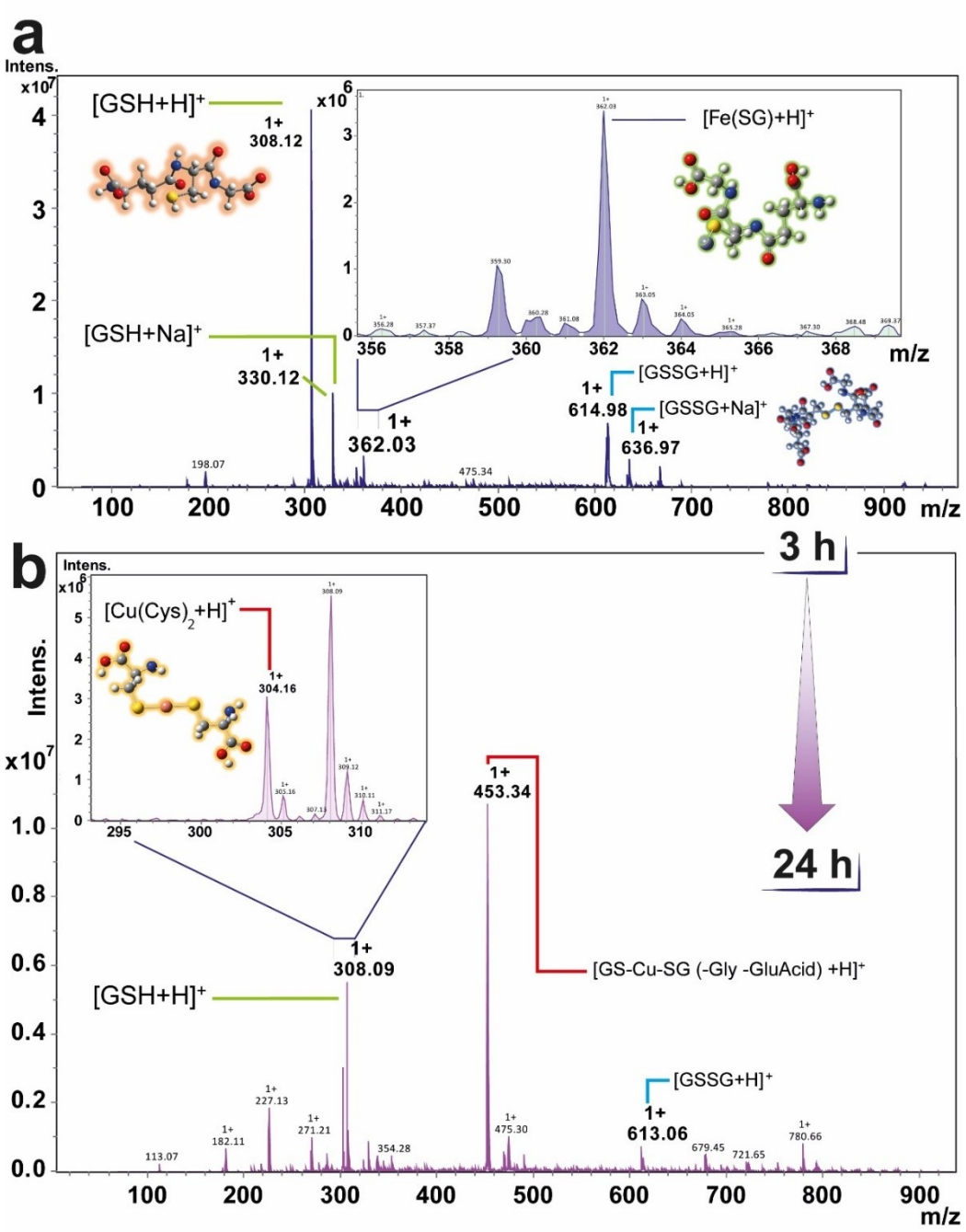

Figure ESI-11. MS-ESI analysis of CuFe+GSH reaction (pH = 3.60) at (a) 3 h and (b) 24 h. $[Fe(SG)+H]^+$ complex formed by Fe leached in the reaction at acidic pH is found at m/z = 362.03. Remaining GSH signal (m/z = 308.19, $[GSH+H]^+$ and m/z = 330.12 $[GSH+Na]^+$) is attributed to slow kinetics of Fe-catalytic oxidation of GSH. Analysis of the reaction at 24 h reveals the generation of $[Cu(SG)_2]^+$ as fragments of $[Cu(cys)_2]^+$ and [Cu(SG)-Gly-GluAcid] appears in the HRMS-ESI at m/z = 304 and 453, respectively.

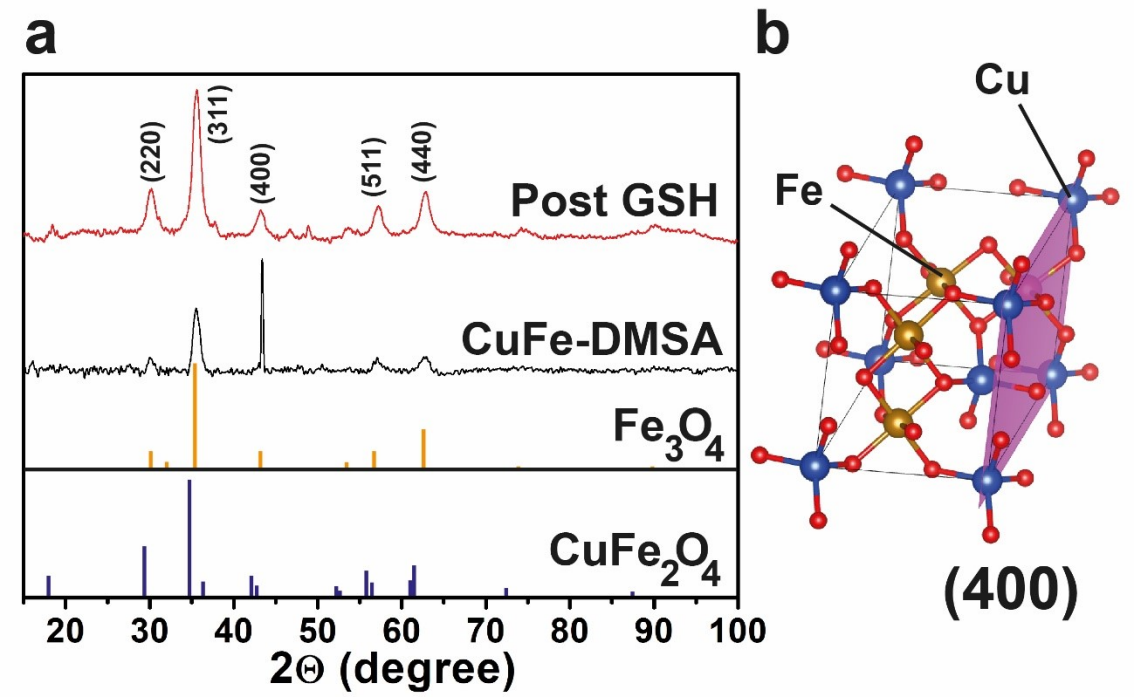

Figure ESI-12. (a) XRD pattern obtained from CuFe-BSA and CuFe-DMSA after reaction with 5 mM of GSH and (b) Cubic structure of $CuFe_2O_4$ where Fe and Cu occupy octahedral and tetrahedral sites, respectively.

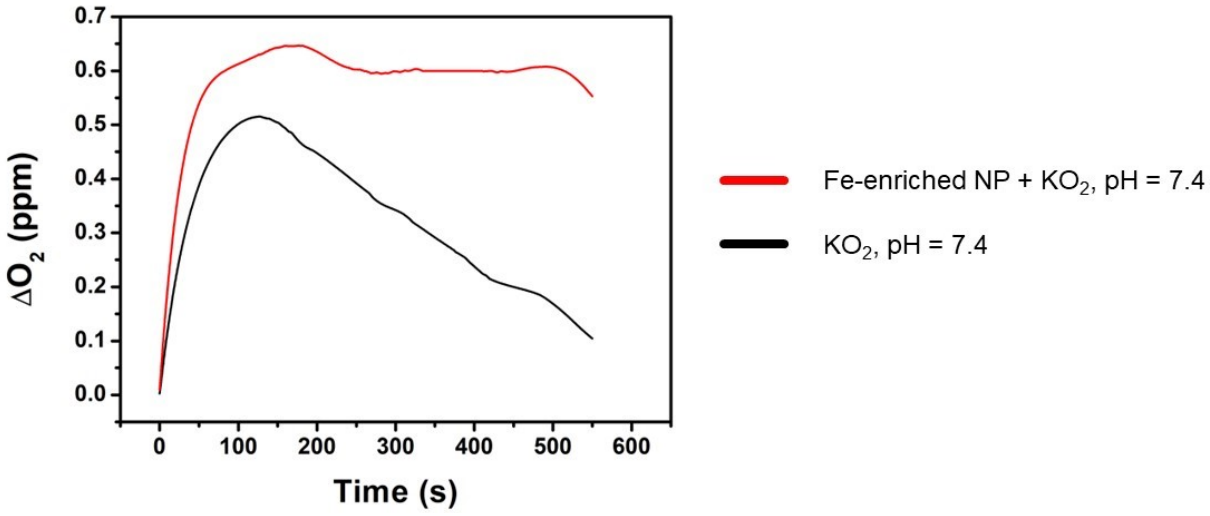

Figure ESI-13. O_2 evolution in the presence/absence of Fe-enriched nanoparticle (red and black line, respectively) using KO_2 as superoxide anion source. The role and influence of the catalyst becomes more evident at longer reaction times in spite of the the rapid self-dismutation of superoxide in reaction conditions (Temperature = 25 ^{o}C, pH = 7.4 (adjusted with Na_2HPO_4/KH_2PO_4 buffer), $[KO_2]_0$ = 100 μM, [Fe-enriched catalyst] = 0.08 mg·mL^{-1}.

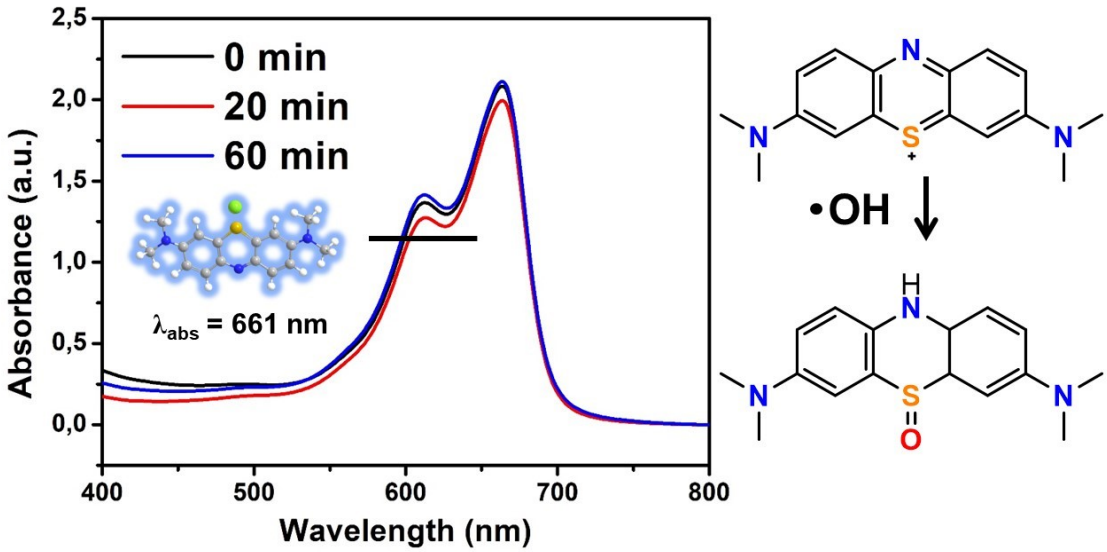

Figure ESI-14. Study of •OH generation from from reaction of Fe-enriched catalyst (0.1 mg·mL^{-1}). UV-vis spectra of Methylene Blue at different times (after CuFe incubation with 5 mM GSH to provoke Cu release) in the presence of H_2O_2 1 mM (T = 25 ºC, pH = 6.5 (adjusted with CH_3COO^- 0.05 M).

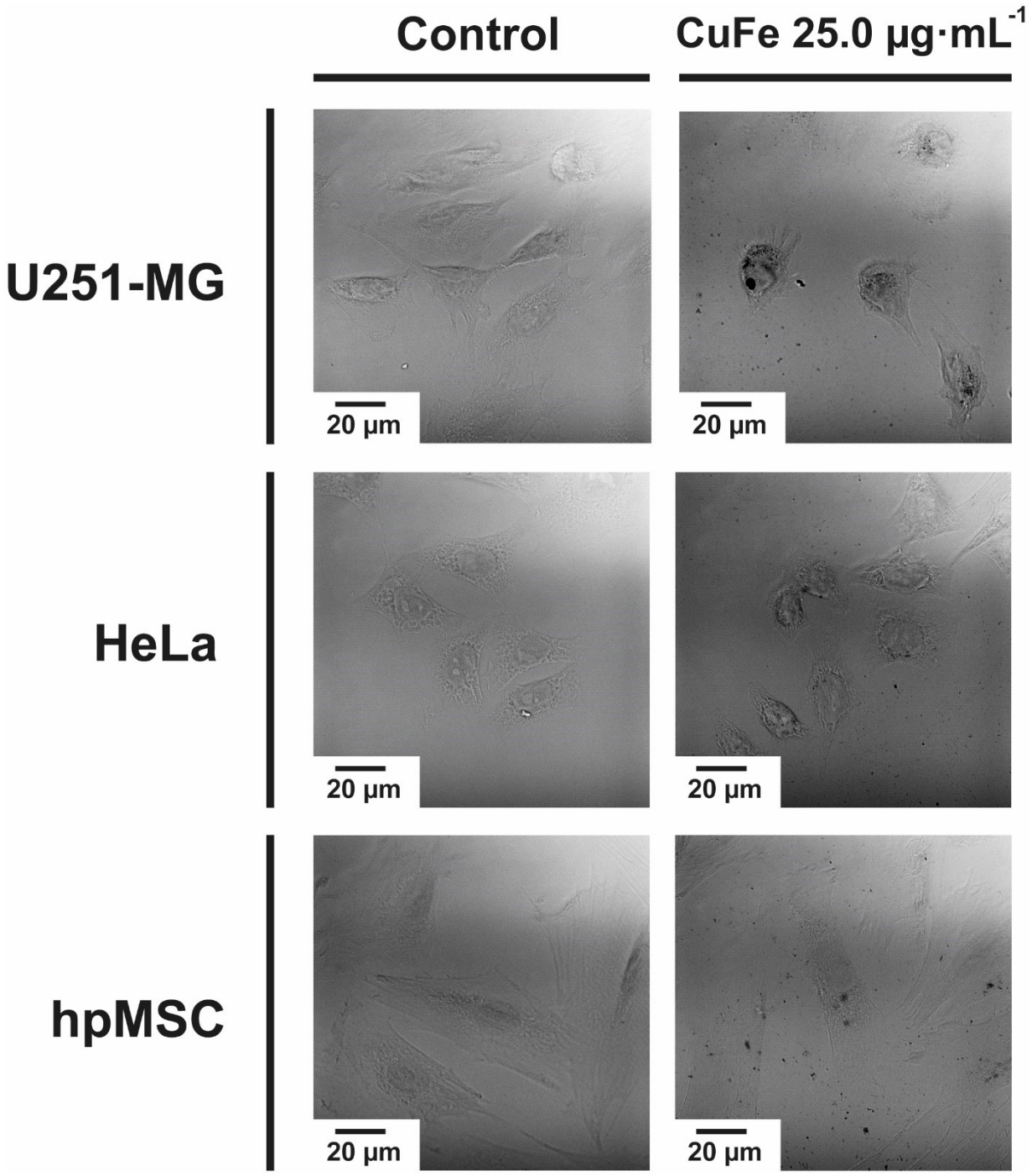

Figure ESI-15. Representative confocal microscopy images of U251-MG, HeLa and hpMSC cell lines treated with 25.0 µg·mL^{-1} after 24h of treatment analyzed through Transmitted Light Detector (T-PMT). The contrast provided by CuFe nanocatalyst aggregates possibilities its visualization within the cells.

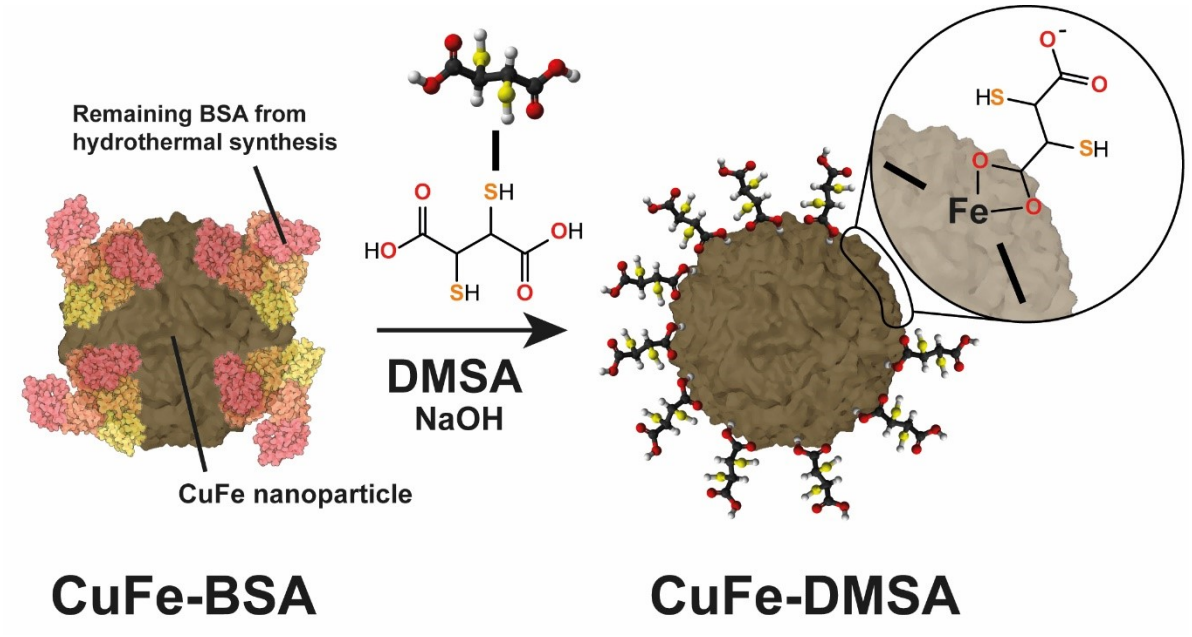

Figure ESI-16. CuFe-DMSA synthesis route. A ligand exchange process is applied to as-synthetized CuFe-BSA nanoparticles to promote the replacement of BSA remaining from the hydrothermal synthesis by DMSA. An alkaline medium is necessary to solubilize DMSA into the aqueous media. Once deprotonated, carboxyl groups from DMSA are able to bind to Fe^{III} sites in the nanoparticle to enhance the dispersion of the nanoparticles in aqueous media.

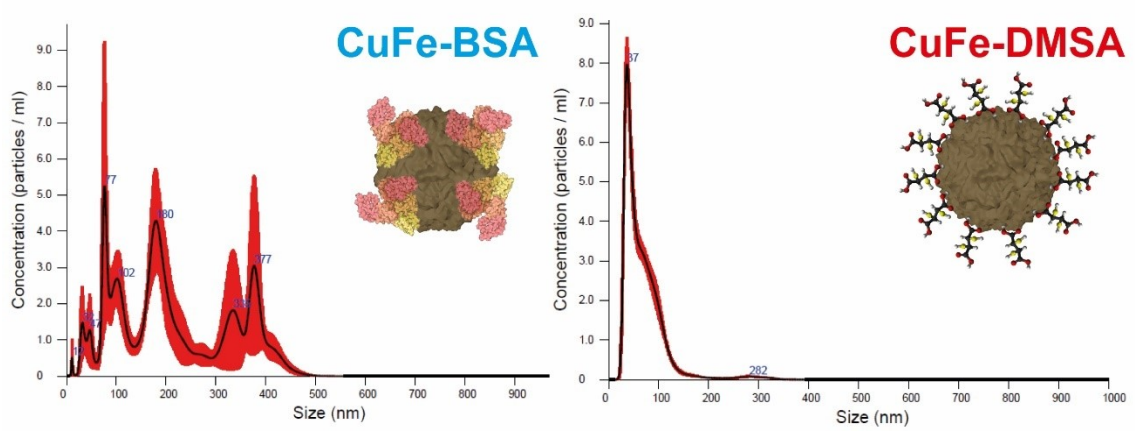

Figure ESI-17. Nanoparticle Tracking Analysis (NTA) of CuFe before (BSA) and after DMSA functionalization, showing the effectiveness of DMSA functionalization to disperse the nanoparticles in aqueous media.

Table ESI-1. Elemental composition of CuFe surface measured by XPS before exposure to GSH

Binding Energy (eV)				
Cu 2p	**Fe 2p**	**O 1s**	**N 1s**	**C 1S**
932.6	710.8	530.4	400.2	285.0
7.80%	18.74%	40.15%	0.81%	32.47%

Table ESI-2. Elemental composition of CuFe surface measured by XPS after exposure to GSH

Binding Energy (eV)				
Cu 2p	**Fe 2p**	**O 1s**	**N 1s**	**C 1S**
932.2	711.2	530.3	400.1	285.0
0.28%	21.00%	44.24%	2.52%	31.96%

Table ESI-3. XPS quantification of the different Fe and Cu species present on the catalyst surface before exposure to GSH

Fe^{2+}		Fe^{3+}	
2p3/2	S.O	2p3/2	S.O
710.6	714.0	712.1	718.4
40%	-	60%	-

$Cu^{0/+}$	Cu^{2+}		
2p3/2	2p3/2	S.O.1	S.O.2
932.6	934.3	941.2	944.2
17%	83%	-	-

Table ESI-4. XPS quantification of the different Fe and Cu species present on the catalyst surface after exposure to GSH

Fe^{2+}		Fe^{3+}	
2p3/2	S.O	2p3/2	S.O
710.9	713.7	711.0	718.6
28.5%	-	71.5%	-

$Cu^{0/+}$	Cu^{2+}		
2p3/2	2p3/2	S.O.1	S.O.2
932.7	934.5	941.2	943.7
59%	41 %		

Table ESI-5. GSH standards composition employed to analyse GSH-catalytic experiments

[GSH] (ppm)	V_{GSH} 100 ppm (μL)	V_{DTNB} 1 mM (μL)	V_{TRIS} 0.01 M (μL)
2.5	25	100	875
5.0	50	100	850
10	100	100	800
20	200	100	700
40	400	100	500

Table ESI-6. CC50 values obtained for CuFe catalyst for different cell lines at different treatment times, expressed in $\mu g \cdot mL^{-1}$

	Fibroblasts	hpMSC	U251-MG	U87	HeLa	SKOV3
24 h	110.7 ± 21.4	113.3 ± 24.6	31.7 ± 9.9	8.6 ± 3.0	47.9 ± 22.3	9.3 ± 2.4
48 h	66.3 ± 17.7	54.5 ± 13.4	9.5 ± 3.5	6.3 ± 1.5	19.8 ± 11.8	6.1 ± 2.0
72 h	83.4 ± 26.1	27.5 ± 7.4	9.5 ± 4.2	6.0 ± 2.0	32.0 ± 6.7	6.6 ± 1.6

Table ESI-7. GSH standards composition employed to analyse intracellular GSH-catalytic experiments

[GSH] (ppm)	$V_{GSH,\ TCA}$ (μL)	$[GSH]_{TCA}$ (ppm)	$V_{DTNB\ 1\ mg \cdot mL\text{-}1}$	$V_{TRIS\ 0.01\ M}$
0.25	50	5	20	930
0.35	50	7	20	930
0.50	50	10	20	930
0.75	50	15	20	930
1.00	50	20	20	930
2.00	50	40	20	930
3.00	50	60	20	930
5.00	50	100	20	930